

An extended *XMM-Newton* observation of the Seyfert galaxy NGC 4051 - III. FeK emission and absorption

K.A.Pounds, S.Vaughan

Department of Physics and Astronomy, University of Leicester, Leicester, LE1 7RH, UK

Accepted ; Submitted

ABSTRACT

An extended *XMM-Newton* observation of the Seyfert 1 galaxy NGC 4051 in 2009 detected a photoionised outflow with a complex absorption line velocity structure and a broad correlation of velocity with ionisation parameter, shown in Pounds et al.(2011) to be consistent with a highly ionised, high velocity wind running into the interstellar medium or previous ejecta, losing much of its kinetic energy in the resultant strong shock. In the present paper we examine the FeK spectral region in more detail and find support for two distinct velocity components in the highly ionised absorber, with values corresponding to the putative fast wind ($\sim 0.12c$) and the post-shock flow ($v \sim 5000\text{--}7000 \text{ km s}^{-1}$). The Fe K absorption line structure is seen to vary on an orbit-to-orbit timescale, apparently responding to both a short term increase in ionising flux and - perhaps more generally - to changes in the soft X-ray (and simultaneous UV) luminosity. The latter result is particularly interesting in providing independent support for the existence of shocked gas being cooled primarily by Compton scattering of accretion disc photons. The Fe K emission is represented by a narrow fluorescent line from near-neutral matter, with a weak red wing modelled here by a relativistic diskline. The narrow line flux is quasi-constant throughout the 45-day 2009 campaign, but is resolved, with a velocity width consistent with scattering from a component of the post-shock flow. Evidence for a P Cygni profile is seen in several individual orbit spectra for resonance transitions in both Fe XXV and Fe XXVI.

Key words: galaxies: active – galaxies: Seyfert: general – galaxies: individual: NGC 4051 – X-ray: galaxies

1 INTRODUCTION

An extended *XMM-Newton* observation of the Seyfert 1 galaxy NGC 4051 in 2009 found a rich absorption line spectrum indicating a photoionised outflow with a wide range of velocities and ionisation parameter (Pounds et al. 2011; hereafter Paper I). The absorption line velocity structure and a broad correlation of velocity with ionisation parameter were shown to be consistent with an outflow scenario where a highly ionised, high velocity wind, perhaps launched during intermittent super-Eddington accretion (King and Pounds 2003), runs into the interstellar medium or previous ejecta, losing much of its kinetic energy in the resultant strong shock.

The wider importance of such shocked outflows lies in the possibility that the accumulated thrust from multiple episodes - rather than the outflow energy - would eventually drive gas from the bulge, thereby limiting further star formation and black hole growth. Such a momentum-driven feedback mechanism has been shown by King (2003, 2005) to

reproduce the observed correlation of black hole and bulge mass (e.g. Ferrarese and Merritt 2000, Gebhardt et al. 2000, Haring and Rix 2004)).

Growing evidence for extreme velocity ($v \sim 0.1\text{--}0.2c$) X-ray outflows (Chartas et al. 2002, Pounds et al. 2003, 2006; Reeves et al. 2003, Cappi 2006, Tombesi et al. 2010) has been confined to the very highly ionised matter ($\log \xi \sim 3.5\text{--}4$) most readily detected in the Fe K band. If the Tombesi et al. findings are confirmed, with highly ionised outflows at $v \sim 0.1c$ being relatively common in bright nearby galaxies, then perhaps Eddington or mildly super-Eddington accretion is also more common than generally believed. (A case for AGN black hole masses being over-estimated has recently been argued by King (2010a)).

We note that if the ejection of fast outflows is intermittent, as suggested in Paper I for NGC 4051, then only where such a wind is current or was launched very recently will it retain a line-of-sight column close to the value $N_H \sim 10^{24} \text{ cm}^{-2}$, appropriate to continuum driving (King and Pounds

2003) and probably required for detection of a $v \sim 0.1c$ flow in a very low redshift AGN with current X-ray missions.

The primary aim of the present paper is to examine the complex Fe K emission and absorption profile of NGC 4051 and attempt to resolve and identify discrete spectral features carrying information on the highly ionised outflow and re-processing of the primary X-ray continuum. We have sought to confirm the presence of the highly ionised pre-shock wind discussed in Paper I, for which scaling from the strong absorption seen at velocities up to $\sim 9000 \text{ km s}^{-1}$ predicts a wind velocity in the range $\sim 0.11\text{--}0.13c$. We also examine the Fe K absorption line structure at different continuum flux levels to establish whether the highly ionised outflow component varies on a similar few-day timescale to that observed in RGS spectra for lower ionisation gas over the same velocity regime (Pounds and Vaughan 2011a; hereafter Paper II).

2 OBSERVATIONS AND DATA ANALYSIS

NGC 4051 was observed by *XMM-Newton* on 15 orbits between 2009 May 3 and June 15. Here we use primarily data from the EPIC pn camera (Strüder et al. 2001), which has the best sensitivity of any current instrument in the Fe K band ($\sim 6\text{--}10 \text{ keV}$). Excluding high background data near the end of each orbit the total exposure available for spectral fitting is $\sim 600 \text{ ks}$. Further details on the timing, flux levels and X-ray light curves for each orbital revolution are included in Vaughan et al. (2011). Line energies are quoted throughout the paper adjusted for the redshift of NGC 4051, with the calculation of line shifts and velocities also taking account of a pn detector energy offset (see below) by cross-reference to the simultaneous data from the MOS camera (Turner et al. 2001). Line widths are the intrinsic values, after allowance for pn camera energy resolution. Unless specified otherwise, uncertainties correspond to 90 % confidence limits.

2.1 Spectral structure in the Fe K region

Figure 1 (top panel) shows EPIC pn spectral data summed over the whole 2009 *XMM-Newton* observation, plotted as a ratio to the continuum determined by first fitting the data between 5 and 10 keV with a power law plus Gaussian emission line at $\sim 6.4 \text{ keV}$, and then removing the line. The aim of that simple procedure was to delineate any emission and absorption fine structure without introducing potential artefacts from modelling the characteristic curvature in the continuum with reflection or ionised absorption.

The ratio plot of pn data to this simple power law continuum shows a narrow Fe K emission line with an apparent red wing, together with several absorption lines to higher energy. Gaussian fitting to the individual spectral features finds the Fe K emission can be modelled with a narrow and a broad component. The narrow line energy (adjusted for the redshift of NGC 4051) is $6.437 \pm 0.006 \text{ keV}$ (¹). The broad

¹ The summed MOS spectrum finds a narrow line energy of $6.409 \pm 0.004 \text{ keV}$, consistent with fluorescence from stationary and cold matter. The MOS energy calibration is believed to be more stable than that of the pn and all absorption line blue-shifts

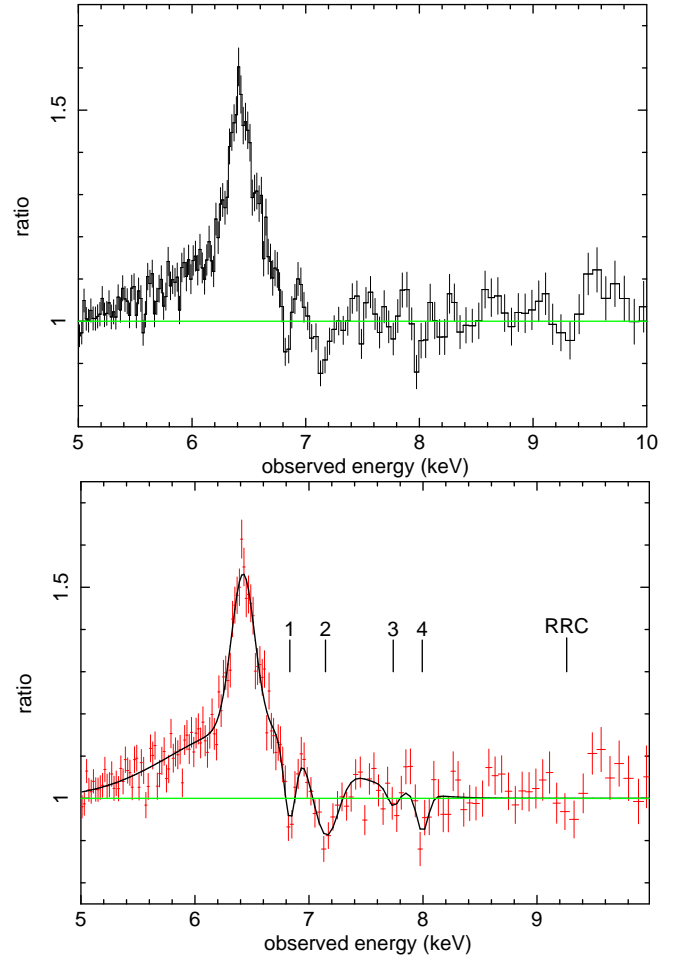


Figure 1. pn data summed over the whole 2009 observation plotted as a ratio to a simple power law between 5 and 10 keV (details in the text). Gaussian fitting in the lower panel models the Fe K emission profile and several possible absorption lines. Details of the Gaussian fits and possible identifications of the absorption lines are listed in Table 1. The zero velocity threshold energy of the putative Fe XXVI RRC is also marked.

component is centred at $6.4 \pm 0.1 \text{ keV}$ with width $\sigma = 650 \pm 70 \text{ eV}$.

Three absorption lines, at ~ 6.8 , ~ 7.15 and $\sim 8.0 \text{ keV}$ and a possible fourth line at $\sim 7.75 \text{ keV}$ were then modelled with negative Gaussians. Lines labelled 1, 3 and 4 in figure 1 were found to be narrow and were therefore fixed at a width corresponding to the pn resolution ($\sigma \sim 60 \text{ eV}$). Component 2 is clearly resolved, and the Gaussian fit yielded an intrinsic 1σ width of $113 \pm 17 \text{ eV}$. Measured line energies (adjusted to the rest frame of NGC 4051) are listed in Table 1 where alternative identifications are used to infer relevant outflow velocities.

Component 1 is rather unambiguously identified with the resonance line of He-like Fe XXV (although a more blue-shifted inner shell UTA is theoretically possible, Kallman et al. 2004). The Fe XXV identification yields a projected outflow velocity of $\sim 5500 \text{ km s}^{-1}$, similar to the strong absorp-

used here to calculate outflow velocities are adjusted by a corresponding factor of 0.996

tion seen in O VIII and higher level ions in the RGS data, and identified with the early post-shock flow in Paper I.

Component 2 has two candidate identifications, the more likely being with H-like Fe XXVI, corresponding to an outflow velocity of $\sim 7200 \text{ km s}^{-1}$ for the measured centroid energy. However, as the line profile is broadened (as it also was in the *XMM-Newton* observation of 2001 (Pounds et al. 2004)), an alternative fit to component 2 is a velocity range $\sim 5000\text{--}9000 \text{ km s}^{-1}$ for Fe XXVI Lyman- α . Interestingly, a similar broad absorption/velocity trough is seen in O VIII Lyman- α in the highest flux RGS spectrum (Paper I).

The third strongest absorption line in figure 3 is component 4, at $\sim 8 \text{ keV}$. The most interesting identification, in the context of the present study, is with Fe XXVI Lyman- α , yielding an outflow velocity of $38300 \pm 1250 \text{ km s}^{-1}$, within the range predicted in Paper I for the pre-shock wind. However, lower velocity absorption from the FeXXV 1s-3p transition must be present at some level, though the relative line strength and low velocity, compared with the 1s-2p line at $\sim 6.8 \text{ keV}$, suggest this may not be the dominant absorption component. Of the remaining candidates listed in Table 1, the Fe XXV 1s-2p line appears least likely, implying an extreme velocity, well outside the predicted range for the putative pre-shock wind, while significant absorption from He-like Ni would imply a substantial over-abundance of Ni relative to Fe.

Finally, if confirmed, component 3 would provide some independent support for the detection of the pre-shock wind, the most likely identification with the Fe XXV resonance line then forming a high velocity pairing with that of Fe Lyman- α for component 4.

The ratio plot of figure 1 also shows a positive feature at $\sim 9.4 \text{ keV}$ lying close to the ionisation threshold energy of Fe XXVI. An intriguing identification, given the strong radiative recombination continua (RRC) seen in the RGS spectrum (Paper II), would be with the RRC of Fe XXVI, with a blue-shifted velocity of $\sim 5300 \pm 2000 \text{ km s}^{-1}$. However, we see in the next Section that the reality of this emission feature is dependent on correctly modelling the underlying continuum near 9 keV .

In summary, a simple examination of pn spectral data summed over the $\sim 600 \text{ ks}$ observation of NGC 4051 finds evidence for several blue-shifted absorption lines in the Fe K band, together with both narrow and broad emission components. The implied outflow velocities from absorption lines 1 and 2, and the indication of line broadening in the feature at $\sim 7.1 \text{ keV}$, maps closely to the velocity profile observed in O VIII Lyman- α and similar lower mass ions (Paper I), suggesting we are seeing in Fe K a co-moving, more highly ionised (lower density) component of the same post-shock flow. Of particular interest in the context of the shocked wind interpretation of the complex RGS absorption spectrum (Paper I, Paper II) is the possible identification of absorption line 4 with Fe XXVI Lyman- α , corresponding to a velocity component with the predicted (factor ~ 4) higher value for the putative pre-shock wind. We note, however, that outcome must be qualified by a likely blend with the 1s-3p transition in Fe XXV.

Table 1. Summary of Gaussian line fits to the four most significant absorption lines in figure 1, adjusted to the NGC 4051 rest frame, and with the corresponding outflow velocity also allowing for the known pn calibration error

line	energy (keV)	ident	velocity (km s $^{-1}$)
1	6.85 ± 0.01	FeXXV (1s-2p)	5500 ± 450
2	7.16 ± 0.015	FeXXV (1s-2p)	17900 ± 650
2	7.16 ± 0.015	FeXXVI Ly- α	7200 ± 650
3	7.76 ± 0.045	FeXXV (1s-2p)	40000 ± 1750
3	7.76 ± 0.045	FeXXVI Ly- α	29800 ± 1750
4	8.01 ± 0.03	FeXXV (1s-2p)	48200 ± 1250
4	8.01 ± 0.03	NiXXVII (1s-2p)	8300 ± 1250
4	8.01 ± 0.03	FeXXV (1s-3p)	3700 ± 1250
4	8.01 ± 0.03	FeXXVI Ly- α	38300 ± 1250

3 FITTING WITH XSPEC

The above procedure, of examining spectral structure in the Fe K band against a simple power law baseline, was adopted to circumvent possible confusion with discrete spectral features that might be introduced in seeking to model the observed curvature in the NGC 4051 broad band spectrum below $\sim 6 \text{ keV}$ and the step function decrease seen above $\sim 7 \text{ keV}$.

To assess such effects and further quantify the emission and absorption line structure in the Fe K spectrum, we have repeated the Fe K profile analysis, but now modelling the underlying continuum with a power law, part of which is attenuated by an ionised absorber, together with a low ionisation reflection component (required for consistency with the narrow emission line at $\sim 6.4 \text{ keV}$). To again avoid the introduction of fine structure into the continuum fit, we model continuum reflection with *pe xriv* (Magdziarz and Zdziarski 1995) and ionised absorption with *absori* (Done et al. 1992), and use the *Xspec* software (Arnaud et al. 1996) to seek an acceptable continuum fit to the EPIC data over the 3-10 keV band. We term this the *prexf* model.

Initial spectral fitting at different flux levels showed the flux of the narrow Fe K line to remain essentially unchanged throughout the 2009 observation, suggesting that a neutral or weakly ionised continuum reflection component should also stay constant. Fitting the 3-10 keV pn spectrum of the lowest flux orbit, rev 1739, with the *prexf* model then provided a measure of that quasi constant reflection continuum. The spectral fit for rev 1739 is reproduced in figure 2, along with the very similar fit for the extended low flux observation in 2002. The *pe xriv* parameters from rev 1739 were then carried forward as a description of the weakly ionised reflection component in fitting the continuum for all 2009 spectra. We focus initially on modelling the summed 2009 pn data, to allow direct comparison with the FeK spectral features obtained in the previous Section.

In modelling the summed pn data the power law index was tied for both absorbed and unabsorbed direct components and for the input to *pe xriv*. Abundances were fixed at solar values and the redshift of the reflected continuum set at that of NGC 4051, as in the fit to the low flux data. The common power law index was left free, as were the normalisations of both direct continuum components, and the column density, ionisation parameter and ‘redshift’ (a proxy for the velocity) of the partial covering absorber.

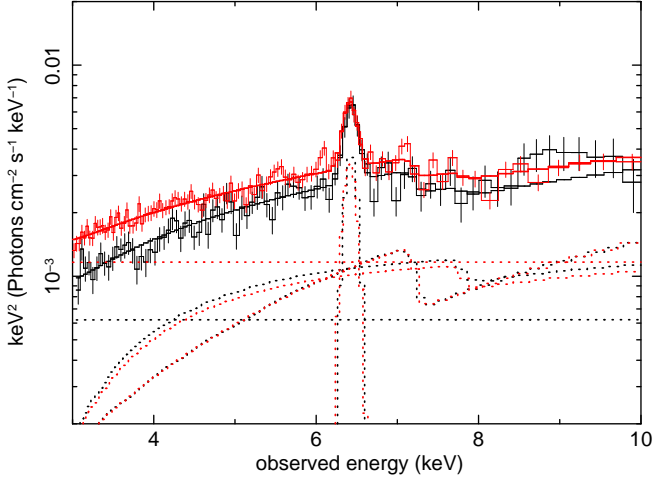


Figure 2. (top) Unfolded spectral fits to the low flux data of rev 1739 in 2009 (black) and rev 0541 in 2002 (red) used here to parameterise the quasi-constant reflection components in the NGC 4051 spectrum

The parameters of the continuum best fit include a tied power law index $\Gamma=1.99\pm 0.01$, close to the value found for the dominant component in a study of broad-band spectral variability (Vaughan et al. in preparation). The continuum reflection, carried over from the low flux fit, is now less dominant in comparison to the direct continuum components, but still contributes significantly to the spectral curvature and provides the step function change seen in the raw data at ~ 7.1 keV. An ionised gas column of $N_H=12\pm 2\times 10^{22}$ cm^{-2} covers $\sim 50\%$ of the direct continuum, with blue shift of 0.026 ± 0.009 and ionisation parameter $\xi=210\pm 17$ erg cm s^{-1} combining to place a (weak) absorption edge near ~ 8 keV.

With the addition of a positive Gaussian to model the narrow Fe K emission line near 6.4 keV, the 3–10 keV spectral fit remained unacceptable, with χ^2 of 1280 for 1017 degrees of freedom. The main residuals are shown in figure 3 (top panel), where the narrow emission line has been re-introduced to allow visual comparison with figure 1. Inclusion of the cold reflection continuum now confines the broad excess emission to the red side of the narrow Fe K line. As the latter is strongly suggestive of a relativistic fluorescent emission component, we then modelled this excess with a *diskline* (Fabian et al. 1989), improving the 3–10 keV fit to χ^2 of 1147/1012. We term this the *pcrefdisk* model and review the emission components in Section 4.

To quantify the residual Fe K spectral structure (figure 3, lower panel) the *pcrefdisk* model was then taken as a baseline, with positive and negative Gaussians added in *Xspec* to model the emission and absorption fine structure. All parameters of the continuum fit (other than for *pcrriv*) were left free in order to quantify the improvement in fit with the addition of each discrete spectral component. The final outcome was an excellent 3–10 keV spectral fit, with χ^2 of 994 for 1000 degrees of freedom. The unfolded spectrum and spectral components are illustrated in figure 4. ⁽²⁾

² To independently test the reliability of detection of absorption lines we used a $\Delta\chi^2 > 11$ criterion, the improvement in the fit expected to occur with a probability $p = 0.01$ (or ‘99 per cent confidence’) when adding a narrow absorption line in the range

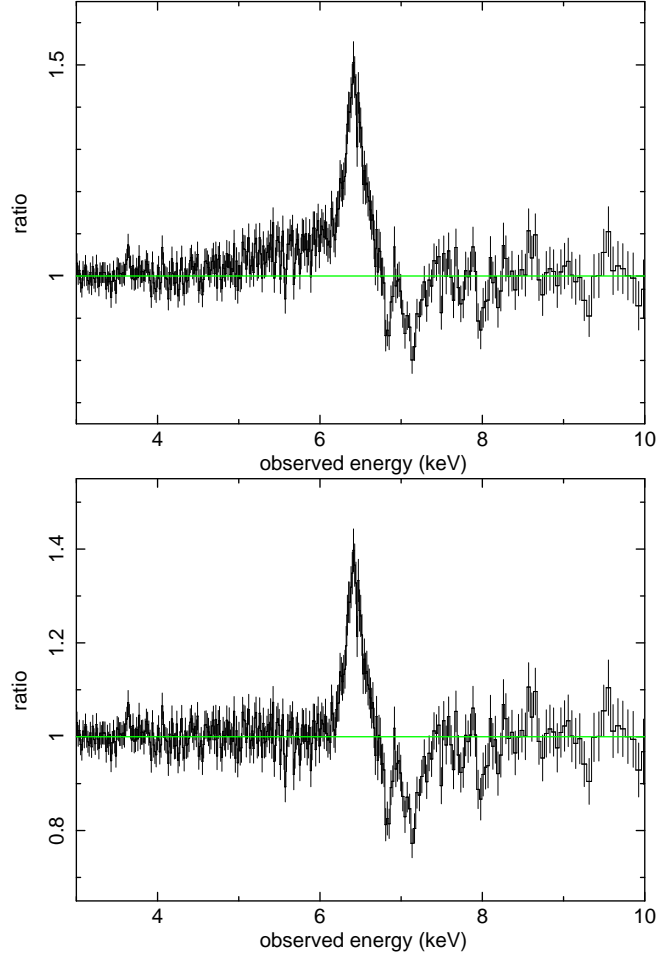


Figure 3. (top) Data residuals for the *pcref* continuum model of the summed 2009 pn spectrum, and (lower) with the addition of a relativistic emission line. Details in the text

The absorption line energy, equivalent width and significance of each absorption line are listed in Table 2. Each line is again unresolved apart from that near 7.15 keV. While that line broadening might be due to imperfect modelling of the *pcrriv* absorption edge, a more interesting alternative is that noted in the previous Section, namely that the line width relates to a spread of outflow velocities, as found in the same post-shock velocity regime in RGS data (Paper I).

In summary, a more physical spectral analysis finds

6.7 – 9 keV, when no such line is present. The p -value was calibrated using a Monte Carlo method. We simulated 1000 EPIC pn source and background spectra with the same exposure time as the summed 2009 spectrum, the spectra being generated using a simple model comprising a power law plus narrow, neutral iron line, with parameters derived from fitting the real data, but randomised using the covariance matrix at the best fit. (The technical details of that procedure are discussed in Hurkett et al. 2008; section 3.2). For each simulated spectrum we fitted the 5–10 keV ranges with the power law model plus emission line, and then inserted a narrow absorption line with centroid energy restricted to the 6.7–9 keV band. For each simulation we recorded the $\min(\chi^2)$ statistic for the two models (line and no line), from which we estimated the sampling distribution of the $\Delta\chi^2$ statistic. A $\Delta\chi^2 > 11$ occurred for only 8 of 1000 simulations.

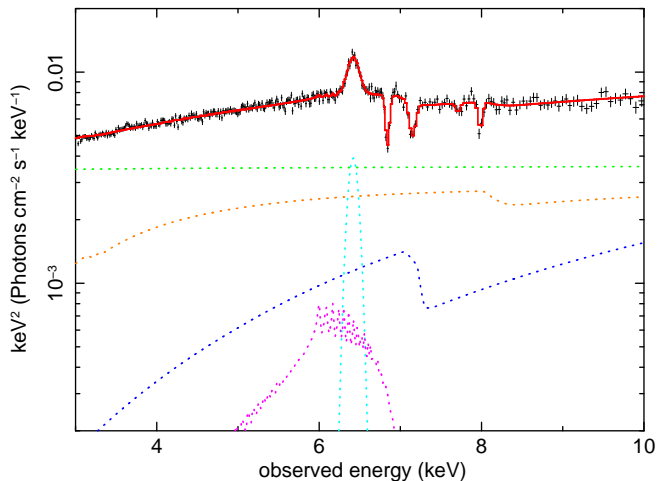


Figure 4. Unfolded spectrum from the broad band fit to the pn data summed over the whole 2009 observation, with the spectral curvature and step function drop in the continuum above 7 keV modelled by a constant reflection component carried forward from the low flux fitting, together with a direct power law component partially covered by a photoionised absorber. The Fe K emission is modelled by a narrow Gaussian line and a relativistic *diskline*. Several absorption lines are required to obtain a good overall fit to the data

Table 2. Summary of Xspec modelling of the absorption line spectral structure shown in figure 3. Line energies are adjusted only for the redshift of NGC 4051, with the corresponding outflow velocity (assuming the preferred identifications with 1s-2p and 1s-3p transitions of Fe XXV and with Fe XXVI Lyman- α) also allowing for the known pn calibration error. Line equivalent widths are determined against the direct continuum, excluding the cold reflector

line	energy(keV)	velocity (km s ⁻¹)	EW(eV)	$\Delta\chi^2$
1	6.86 \pm 0.01	5500 \pm 500	-34 \pm 5	43
2	7.17 \pm 0.03	7300 \pm 1600	-50 \pm 5	80
3	7.74 \pm 0.08	39100 \pm 3200	-11 \pm 5	7
4	8.00 \pm 0.05	3400 \pm 1500	-23 \pm 5	19
4	8.00 \pm 0.05	37900 \pm 1500	-23 \pm 5	19

absorption lines 1, 2 and 4 to be detected at high significance, with line 3 at $\sim 2\sigma$. On the critical question of the identification of line 4, support for detection of the putative pre-shock wind is strengthened by the better agreement between the derived (high) velocities for components 3 and 4, while the EW ratio of 1.5 ± 0.5 for components 1 and 4 is inconsistent with the (optically thin) ratio of 5.2 for FeXXV alone. The velocities obtained from components 1 and 2 remain marginally inconsistent; however, that difference may be real, if the highly ionised post-shock flow component has a velocity/ ionisation gradient similar to that found in the RGS data (Paper I).

4 FE K EMISSION

The broad band spectral fitting in the previous section modelled the Fe K emission with a narrow Gaussian component and a relativistic *diskline* (Fabian et al. 1989). The narrow

component (when adjusted for the pn calibration shift) lies close to 6.4 keV, with an equivalent width (EW) against the direct continuum of ~ 110 eV, consistent with fluorescence from the weakly ionised reflector in the continuum fit (Matt 2002). Finding parameters of the narrow emission line in the summed data consistent with those for the low flux orbit, rev 1739, is strong support for our initial assumption that the cold reflection component was essentially unchanged during the 2009 campaign. However, the line appears resolved, with an intrinsic width $1\sigma = 70\pm 10$ eV. If due only to velocity broadening, that width corresponds to $\sim 7500\pm 1100$ km s⁻¹ (FWHM), intriguingly close to the dominant velocity in the post-shock outflow.

Relativistic fluorescence emission from the inner accretion disc is a reasonable candidate for the red wing of the Fe line, given that the rapid flux variability in the X-ray emission from NGC 4051 (Vaughan et al. 2011) indicates a primary continuum source dimension of a few $10R_G$. The 3-10 keV spectral fit described in the previous Section includes a *diskline* with an input line energy of 6.8 ± 0.2 keV, emissivity index $\beta = -4.5\pm 0.7$, $R_{in} = 6\pm 1$ and inclination of $23\pm 3^\circ$. The line is relatively weak, with EW ~ 130 eV.

Although the narrow emission line appears quasi-constant throughout the 2009 observation, we cannot assume that is also true for the *diskline* component. That issue is raised in the following Section when we explore the variability of the Fe K profile and find evidence for PCygni emission associated with the stronger absorption lines. If confirmed, that would confirm a substantial covering factor in the ionised flow (as was found previously for the high velocity outflow in the luminous Seyfert PG1211+143; Pounds and Reeves, 2009).

5 SHORT TERM VARIABILITY IN THE FE K PROFILE

The Fe K absorption line spectrum in the summed 2009 data is more complex than the single ~ 7.1 keV absorption line reported from the 2001 *XMM-Newton* observation (Pounds et al. 2004). In particular, a second strong absorption line at ~ 6.8 keV supports the 2001 line identification with Fe XXVI Lyman- α , for a velocity of ~ 6500 km s⁻¹ (in preference to Fe XXV 1s-2p and a velocity of ~ 17500 km s⁻¹), with a similar outflow velocity but somewhat lower ionisation parameter in the summed data from 2009. A coordinated *Chandra* and *Suzaku* study 6 months before our 2009 *XMM-Newton* campaign also found absorption lines at ~ 6.8 and ~ 7.1 keV (Lobban et al. 2010), perhaps suggesting little change in the highly ionised ~ 6500 km s⁻¹ outflow component over that timescale.

However, our analysis of the RGS data from the 2009 *XMM-Newton* observation (Paper I, Paper II) found evidence for a change in the ionisation state of more moderately ionised gas on a timescale of a few days. As the two strongest absorption lines in the Fe K region indicate a comparable (~ 5000 - 7000 km s⁻¹) velocity regime, it is interesting to check for a similarly rapid response to changes in the incident continuum flux level. More particularly, if the Fe XXV and XXVI absorption arises in a co-moving, lower density (and more highly ionised) flow component, we might antici-

pate measurable variability over the 6-weeks duration of the 2009 observation.

To search for short-term variability in the Fe K profile we have used the summed 2009 data fit described in Section 3 as a template against which to compare spectral fits for individual orbits. The cold reflection and narrow Fe K emission line parameters were fixed in this comparison, but the power law index and normalisations, *diskline* normalisation and ionisation parameter of the partial cover were left free. The energy and width of the individual absorption lines were fixed at the summed data values, implying no short-term change in the velocity structure of the outflow. Fitting was carried out for individual orbit data over 3-10 keV.

Figure 5 plots the equivalent width (EW) of the 4 absorption lines of figure 4 and Table 2, together with the 0.3-3 and 7-10 keV luminosities, for successive orbits rev1721 (1) to rev 1743 (15), with the summed spectral fit as (16). The single orbit parameters were then compared to the best fitting constant value, using a χ^2 test in order to quantify evidence for their variability. In three cases (~ 6.8 , ~ 7.1 and ~ 8.0 keV) the EWs were found to be variable at greater than 99% confidence. Visual examination of figure 5 suggests the individual absorption line EWs vary in a non-random manner. In particular, the ~ 6.8 and ~ 8.0 keV absorption depths both appear to increase over the first 4 orbits, and follow a visually similar pattern over the remaining orbits. Since the strong ~ 7.1 keV absorption line does not follow the same pattern, the implication is of a change in ionisation state, rather than column density, in the corresponding velocity component of the (post shock) outflow.

To test those impressions we searched for correlations between the absorption line EWs and continuum luminosities, using the standard Pearson (linear) correlation coefficient. The four absorption lines were compared to each other and to the 7-10 keV and 0.3-3 keV luminosities. The only strongly significant correlation (at $\gtrsim 99\%$ confidence) was found between the EWs of the ~ 6.8 and ~ 8.0 keV absorption lines. Over the whole data set the ~ 6.8 and ~ 7.1 keV lines were not significantly correlated, while none of the lines showed a significant correlation to the continuum flux. However, visual inspection of figure 5 does suggest a link of EWs with extreme continuum values on an orbit-to-orbit timescale, and similar trends over several adjacent orbits. While these findings are not simply understood, the lack of a strong correlation with continua levels overall may indicate a delayed response to the ionising flux for both the high and lower velocity (putative pre- and post-shock) flow components, or - as indicated below - a competition between hard ionising radiation and soft Compton cooling flux.

The inter-line correlations are not decisive on the identification of the ~ 8 keV absorption. While the ~ 6.8 and ~ 8.0 keV absorption depth correlation is expected if both lines are from FeXXV, the similar EWs would require the 1s-2p resonance absorption to be strongly saturated, inconsistent with its marked variability. In addition, a positive correlation with the most likely alternative candidate for line 4, namely a high velocity component in Fe Lyman- α , could also arise if the mean ionisation states of the post-shock and pre-shock flow components lie, respectively, between Fe XXV/ Fe XXVI and Fe XXVI/XXVII. Comparison with a photoionisation grid shows that situation implies a difference in ionisation parameter for the two flow components in

the range $\sim 6-8$ (Kallman et al. 2004), qualitatively consistent with the factor 4 increase in density of the flow across a strong shock, followed by a further increase as the post-shock flow slows to ~ 5500 km s $^{-1}$ (Paper I). The continuum driving model for high velocity AGN winds (King and Pounds 2003) would predict such an extreme launch ionisation parameter.

5.1 Individual orbit spectra in 2009

We review below some individual-orbit spectra with the aim of clarifying the apparent variations in ionisation state of the absorbing outflow, and find additional orbital timescale changes in emission. Figure 6 shows the best-fit Fe K profiles for the first 8 orbits (rev 1721 to rev 1730) of the 2009 *XMM-Newton* campaign. Orbit-to-orbit differences are seen in both absorption and emission structure.

At top left the mean profile for the summed 2009 pn data is reproduced, noting - in particular - similarly strong absorption lines at ~ 6.8 and ~ 7.1 KeV. In contrast, the sum of the first two orbits, revs 1721 and 1722 (similar individual orbit profiles have been added in figure 6 for improved definition) shows the 7.1 keV line to be dominant. However, by the next observation, rev 1724, the situation has reversed with the 6.8 keV line now the stronger. Identifying this line pair, as before, with resonance absorption in Fe XXV and Fe XXVI, respectively, indicates the ionisation state of the relevant outflow component, at $v \sim 5000-7000$ km s $^{-1}$, has fallen over that 4 day interval. Figure 5 shows the 7-10 keV luminosity *rising* over those early orbits, which rules out a simple link with the ionising continuum $\gtrsim 7$ keV, unless there is a substantial recombination time delay in the relevant outflow component after some (unseen) high flux level prior to the first *XMM-Newton* observation.

However, figure 5 does show those first 3 orbits to be on a stronger rising trend in soft X-ray flux, the 0.3-3 keV flux doubling from rev 1721 to rev 1724, offering an alternative explanation of the change in ionisation state which is qualitatively consistent with dominant Compton cooling of the post-shock gas, as proposed in Paper I. The broad range of ionisation parameter over which the He-like ion stage is dominant might then explain the similar absorption profile being maintained as the overall continuum flux falls in rev 1725. The Compton cooling interpretation is supported by the following (rev 1727) profile, where the 6.8 KeV absorption line remains dominant, and where figure 5 shows the soft X-ray luminosity to be still higher. The rev 1727 profile also shows a strong emission shoulder to the high energy side of the narrow Fe K line. We return to considering that emission feature in Section 5.2.

The 6th panel in figure 6, for revs 1728 and 1729 (again similar individual orbit profiles have been added) shows the ionisation state to have recovered to that of the summed data, while the 0.3-10 keV luminosity has fallen by over a third from the high rev 1727 value, with the ionising continuum (7-10 keV) luminosity remaining little changed. The new trend of increasing ionisation parameter is extended in rev 1730, with the 7.1 keV line now dominant. Although the soft X-ray luminosity has again increased in rev 1730, figure 5 shows this is the only orbit for which the 7-10 keV luminosity is significantly above the mean value. We suggest later that the factor ~ 2 increase in ionising flux in rev 1730,

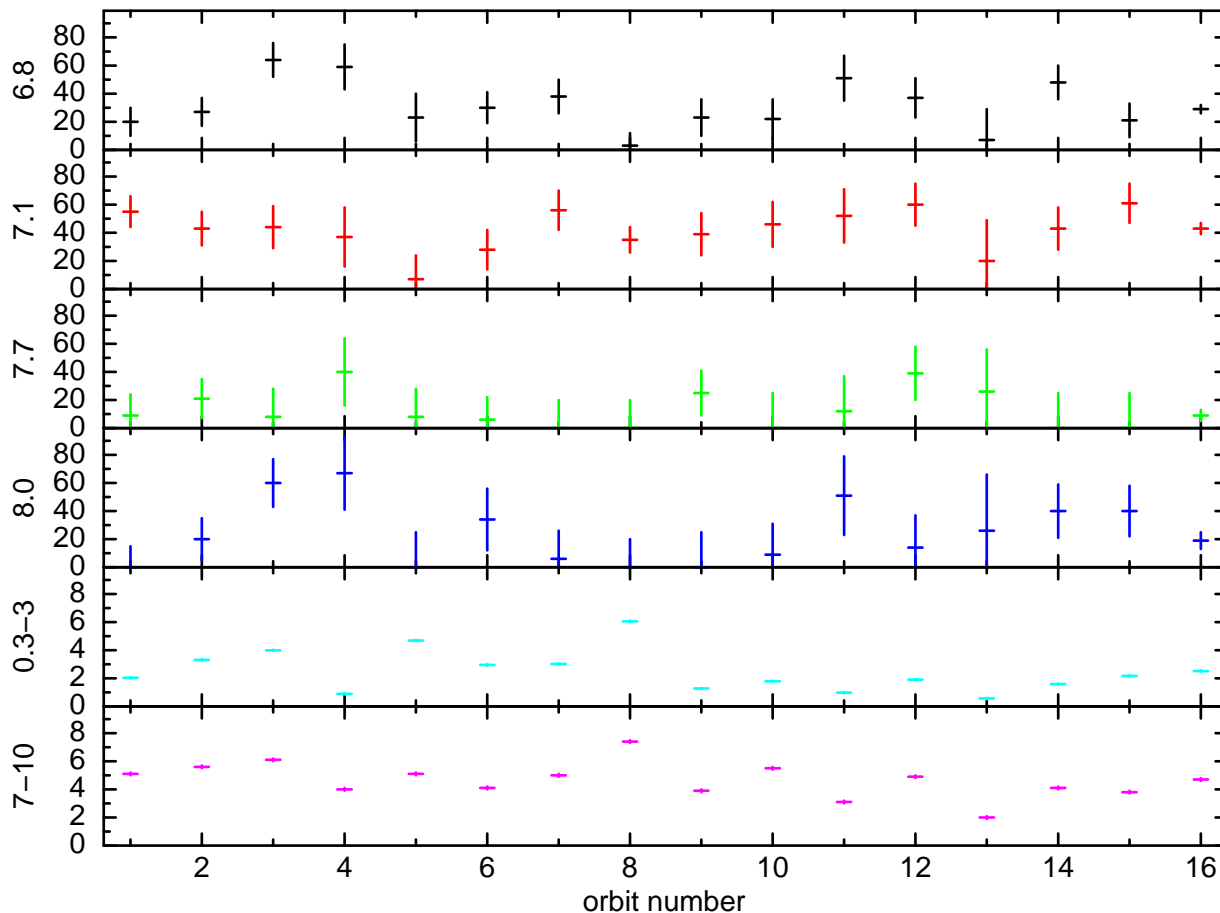


Figure 5. Short term variation in the equivalent width of the 4 strongest absorption lines compared with the 0.3-3 keV luminosity (in units of 10^{41} erg s^{-1}) and 7-10 keV luminosity (units of 10^{40} erg s^{-1}), obtained by fitting individual orbit spectra to the template derived from modelling the summed 2009 data

the highest of the campaign, is the probable cause of this highly ionised state.

The final panel in figure 6 shows the Fe K profile for rev 1736, where the X-ray continuum has again fallen to a low value, very similar to that of rev 1725. The absorption spectrum is also very similar to rev 1725, with a dominant line at ~ 6.8 keV indicating the ionisation state of the ~ 6500 km s^{-1} flow component is again below the 2009 mean.

5.2 The unusual Fe K profile of rev 1727

The Fe K profile for rev 1727, coincident with an unusually strong soft X-ray flux, is particularly striking, and notably different from that for the summed 2009 data. While only the ~ 6.8 keV absorption line can be seen, P Cygni emission is clearly visible on the low energy shoulder of that line. ⁽³⁾ Adding positive and negative Gaussians to model the P Cygni structure (figure 7) yields a significantly improved fit, with $\Delta\chi^2$ of 21 for 5 fewer d.o.f. The absorption line at 6.81 ± 0.02 keV is unresolved (and then fixed at the pn resolution) while the emission component has a 1σ width of 115 ± 38 eV and energy 6.71 ± 0.05 keV. The two components

are of similar EW, indicating a substantial covering factor, with an inflection point at 6.76 ± 0.04 keV, consistent with the rest energy of the Fe XXV 1s-2p resonance transition in the rest frame of NGC 4051. Although not well constrained, the emission line width is also compatible with a wide angle outflow for the ~ 6000 km s^{-1} velocity component, associated in our model with the post-shock gas. We note the potential of higher quality data of such features in mapping the geometry of the correspondingly flow components.

To the low energy side of the Fe line in the rev 1727 data both positive and negative spectral features can be seen, each of which is marginally significant, with $\Delta\chi^2$ of 6 to 8. Those at ~ 5.1 and ~ 5.5 keV might be related to the emission line reported by Turner et al. (2010); see also Section 6. Similarly, absorption lines indicated at ~ 5.35 and ~ 5.75 keV could correspond to the anticipated in-fall of cool, shocked gas with velocities of order $0.2c$ and $0.11c$, respectively. However, unlike the absorption line at ~ 6.8 keV, these lower energy features in the rev 1727 profile do not appear in the spectrum summed over the whole 2009 observation, suggesting they are short lived features or outlying statistical fluctuations.

³ An alternative possibility not explored further here is that the diskline parameters have changed to give a more sawtooth profile.

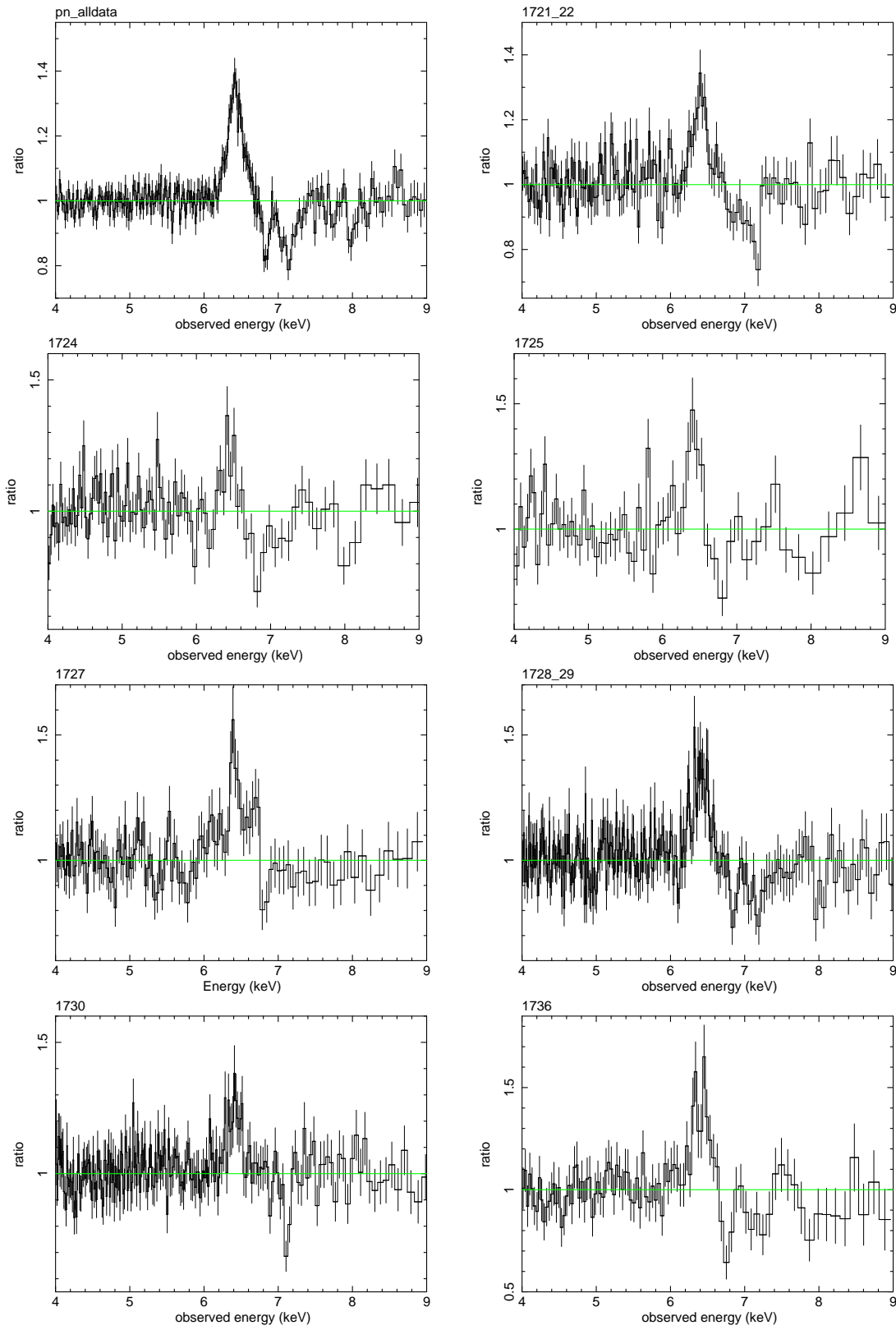


Figure 6. Fe K profiles for the first half of the 2009 *XMM-Newton* campaign (rev 1721 to rev 1730) and a further low flux observation (rev 1736)

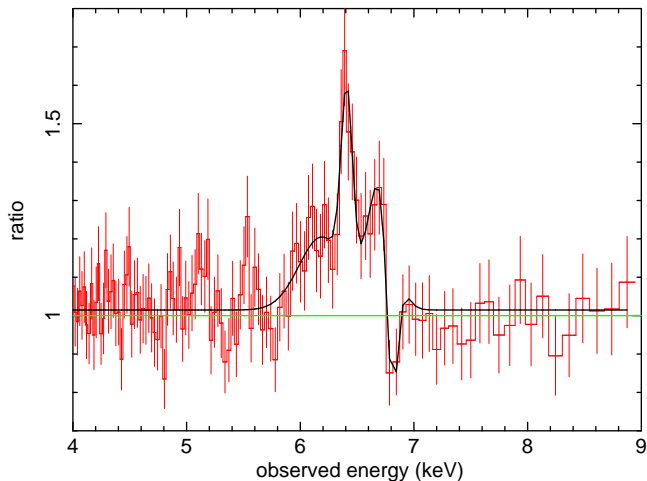


Figure 7. The Fe K profile for rev 1727, coinciding with a strong soft X-ray (and UV) flux, is notably different from that for the summed 2009 data, with only the lower energy absorption line at ~ 6.8 keV clearly seen and visual evidence for P Cygni emission. The figure includes positive and negative Gaussians to model that profile

6 ANOTHER LOOK AT THE 2001 AND 2002 *XMM-Newton* PN DATA

Pounds et al. (2004) previously reported on the *XMM-Newton* observations of NGC 4051 in 2001 and 2002, when the source was in high- and extended low-flux states, respectively. The EPIC spectrum from 2001 (rev 0263) showed a single absorption line at ~ 7.1 keV in both pn and MOS data, with alternative identifications of Fe XXVI Lyman- α and Fe XXV 1s-2p resonance transitions indicating a corresponding outflow velocity of ~ 6500 or ~ 16500 km s $^{-1}$. A comparison with the 2009 summed data template, with only the direct power law and absorption line depths free (a prior check showing the narrow Fe K emission line flux, hence cold reflection, to be only marginally higher), yielded an excellent 3-10 keV fit ($\chi^2 = 582/610$). Figure 8 (top panel) reproduces the ratio plot of the pn data, confirming a dominant, broad absorption line at ~ 7.1 keV.

A fit to the 2002 *XMM-Newton* observation (rev 0541), taken after a 2-week period of unusually low X-ray emission (Uttley et al. 2003), was seen in Section 3 to be very similar to that of the lowest flux orbit (rev 1739) in 2009. Figure 8 (lower panel) shows the Fe K profile from rev 0541, derived at above, dominated by a narrow Fe K- α emission line at $\sim 6.43 \pm 0.01$ keV. Once again, the line is resolved, with width $\sigma = 85 \pm 10$ eV. A statistically significant detection of the Fe K- β line at ~ 7.1 keV finds an EW a factor ~ 5 lower than that of Fe K- α .

The rev 0541 fit is further improved with the addition of a narrow emission line at 5.54 ± 0.02 keV ($\Delta\chi^2$ of 10/2) and an unresolved absorption line at 8.10 ± 0.1 keV ($\Delta\chi^2$ of 8/2). The former feature lies close to that reported at 5.44 ± 0.03 keV in *Suzaku* data and attributed to spallation of Fe into Cr (Turner and Miller 2010). The high energy absorption line was picked out in the survey for high velocity flows in AGN spectra from the *XMM-Newton* archive search by Tombesi et al. (2010), and identified there with Fe Lyman- α for a blue-shifted velocity of $\sim 0.13 \pm 0.01c$.

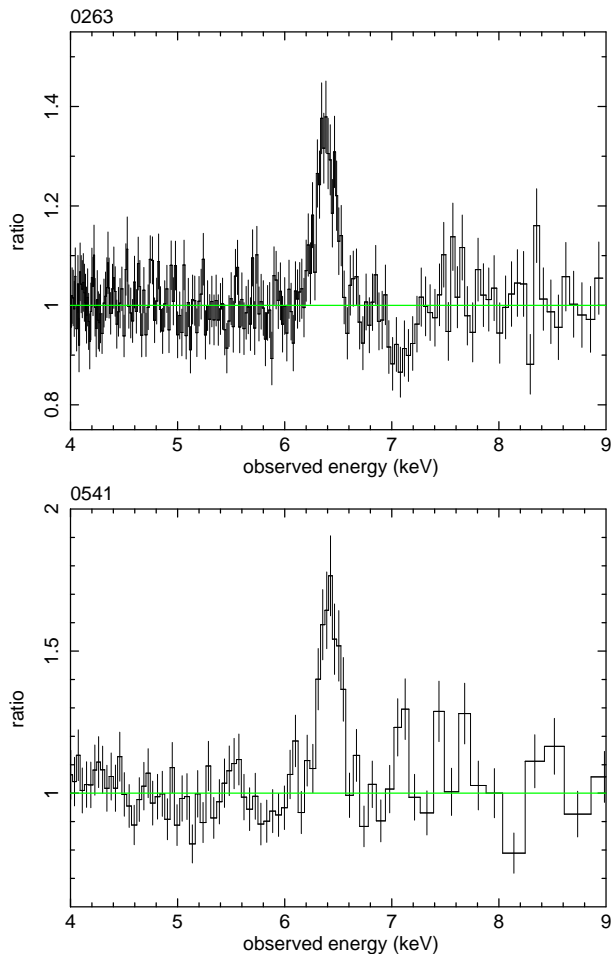


Figure 8. The Fe K profile for the 2001 *XMM-Newton* observation shows a single broad, blue-shifted absorption line with excess flux to the low energy side of the absorption line hinting at a P Cygni line arising from an outflow seen in Fe XXVI Lyman- α . The Fe K profile for rev 0541 is dominated by a narrow emission line at ~ 6.4 keV, with previously reported features in emission at ~ 5.54 keV and absorption at ~ 8.10 keV also found to be significant

In the context of alternative identifications of the ~ 8 keV absorption line in the present paper, it is interesting to note that no absorption line at ~ 6.8 keV is apparent in the rev 0541 spectrum, while being consistent with the putative high speed wind being very highly ionised, becoming more visible in the Fe XXVI Lyman- α line at low ionising fluxes.

In summary, a re-examination of the 2001 data strengthens the earlier interpretation of the line observed at ~ 7.1 keV as arising from Fe XXVI resonance absorption from matter outflowing at ~ 6500 km s $^{-1}$. In the context of our analysis of the more comprehensive absorption data from the 2009 *XMM-Newton* spectra, that finding suggests the post shock flow is persistent, with an ionisation state changing from dominantly Fe XXV to dominantly Fe XXVI as the ionising flux increases to the levels seen in rev 0263 (and rev 1730). The similarity of the narrow FeK emission line flux and (resolved) line width in the 2001, 2002 and 2009 *XMM-Newton* observations suggests the longer-term persistence of the weakly ionised matter responsible for the Fe K line fluorescence and associated continuum reflection. If

that matter is linked to the post shock flow in NGC 4051, as suggested here, the important implication is that the high speed wind is also a persistent feature.

7 DISCUSSION

The 600 ks observation of NGC 4051 in 2009 has provided some of the richest X-ray spectra to date for studying the outflow properties in an AGN. In addition to the increased sensitivity afforded by the unusually long observation, comparison with previous observations from *XMM-Newton*, *Chandra* and *Suzaku* (Collinge et al. 2001, Pounds et al. 2004, Steenbrugge et al. 2009, Lobban et al. 2011) suggests that our 2009 campaign benefited from an overall timescale compatible with intrinsic variability in the flow parameters.

In Paper I we identified 3 broad velocity regimes in the outflow in line-of-sight to NGC 4051, referred to there as the low ($\leq 1000 \text{ km s}^{-1}$), intermediate ($\sim 3000\text{-}9000 \text{ km s}^{-1}$) and high velocity ($\sim 0.1c$) flows, with the low and intermediate velocities well populated by absorption lines from a wide range of metal ions from C to Fe. The highest velocity component was only detected - at relatively low confidence - in Fe K absorption.

Paper I then explored the possibility that the three velocity regimes represent different stages in a shocked high speed wind (King 2010), where the intermediate velocity/intermediate ionisation outflow corresponds to the immediate post-shock gas and the low velocity/low ionisation absorption to matter building up ahead of the contact discontinuity. In a second paper (Paper II), we proposed that a low velocity absorption component observed in RGS spectra near the line cores of several broad resonance emission line components had a separate origin as self-absorption in the limb-brightened shell of shocked gas.

In the King (2010) model a high velocity ionised wind collides with the ISM of the host galaxy, resulting in a strong shock. The gas density increases by a factor ~ 4 at the shock front, and the velocity drops by the same factor. Beyond this (reverse, adiabatic) shock, the flow is further compressed in a relatively thin, cooling region, while the velocity slows to low values at the interface with the ISM. Strong Compton cooling by the AGN soft X-ray/UV radiation leads to a fairly rapid transition between the immediate post-shock regime and the much slower and compressed state near the contact discontinuity.

The primary aim of the present paper has been to examine the complex Fe K emission and absorption profile and attempt to resolve and identify spectral features carrying information on the highly ionised outflow and re-processing of the primary X-ray continuum. We have employed two methods of analysis, first with Gaussian fitting of the ratio for the summed pn data profile to a simple power law baseline, and then by a more physical modelling in *Xspec* where the continuum is fitted with a weakly ionised reflection component (consistent in strength and ionisation state with the observed narrow Fe K fluorescence line), and a partially covered direct power law.

We find the absorption line structure from the two methods to be in good agreement. Detection of 3 (or 4) blue-shifted absorption lines provides evidence for two ve-

locity components in the highly ionised outflow, with a factor ~ 4 difference in velocity as predicted for a shocked flow, although the high velocity component is probably blended with the Fe XXV 1s-3p line. An apparent broadening of the absorption line at $\sim 7.15 \text{ keV}$ (identified with Fe Lyman- α and a outflow velocity range of $\sim 5000\text{-}9000 \text{ km s}^{-1}$) is found in both analysis methods, notwithstanding the proximity of the Fe K absorption edge in the broad band fit. The similarity to the broad absorption trough seen in the RGS data for oxygen Lyman- α (Paper II) again indicates matter of differing densities in a co-moving, decelerating flow.

Our analysis fits the excess flux in the $\sim 5.5\text{-}7 \text{ keV}$ interval with a narrow Fe K emission line and a weak relativistic red wing. We note that the higher resolution (but lower sensitivity) *Chandra* HETG spectrum in Lobban et al. (2011) finds a ‘narrow’ line component almost a factor two broader than in our analysis, although a second fit with an unresolved core underlines the limitation of such simple Gaussian fits. What is interesting is that both Lobban et al. and our present analysis find a substantial Fe K flux arising from weakly ionised matter with a projected velocity dispersion of order $\sim 10^4 \text{ km s}^{-1}$ (FWHM). An appealing interpretation is that this component arises from continuum X-ray flux being scattered from the post-shock outflow, the velocity width implying a wide angle flow.

Comparison of individual orbit spectra with that of the summed data finds the ionisation state of the post shock flow, as determined by the ratio of line opacities of Fe XXVI to Fe XXV, is seen to fall over the first 5 orbits of the 2009 campaign, while the 7-10 keV luminosity, a proxy for the ionising flux affecting the Fe K shell, varies very little. On the other hand, the 0.3-3 keV luminosity increases from rev 1721 to rev 1727 by a factor ~ 2.3 , and simultaneous UV flux measurements show a similar increasing trend (Alston et al. 2012), suggesting the observed ionisation change is responding to enhanced cooling, with a lower gas temperature and corresponding increase in recombination rate. Following that reasoning we can then understand the subsequent reversal to a higher ionisation parameter for the same flow component in revs 1728 and 1729, where the 0.3-3 keV luminosity has fallen back by \sim a third. If confirmed, the above interpretation of the absorption line variations over the first half of the 2009 *XMM-Newton* campaign provides independent support for the shocked outflow model discussed in Paper I, where strong cooling of the post-shock flow is a key to the ionisation-velocity correlation seen in the RGS spectra.

However, while the soft X-ray flux has again increased by rev 1730, that observation sees the largest ionising flux of the campaign, with the 7-10 keV luminosity a factor ~ 2 higher than in rev 1729. The dominant 7.1 keV absorption line, also seen in the similarly high flux observation of 2001 (rev 0263), indicates a still higher ionisation parameter for the $\sim 5000\text{-}7000 \text{ km s}^{-1}$ flow component, with photoionisation now dominating over Compton cooling. If the line ratio change from rev 1729 to rev 1730 is indeed due to an ionising pulse, the ~ 2 day timescale is much shorter than for an ionising front travelling at the local sound speed ($\leq 1000 \text{ km s}^{-1}$) through the shell of post-shock gas, estimated in Paper I to be of thickness $\sim 10^{16} \text{ cm}$. Alternatively, for an R-type ionisation front, moving into a low density medium, the response time will be governed by the recombination time. For an assumed post-shock temperature of $\sim 0.1 \text{ keV}$

(Paper I), a recombination coefficient of 3.5×10^{-11} (Verner and Ferland 1996) would then relate the measured recombination timescale of $\sim 2 \times 10^5$ s to a mean (electron) density of $\sim 1.5 \times 10^5$ cm $^{-3}$.

That value is consistent with the measured absorption column of $N_H \sim 2 \times 10^{21}$ cm $^{-2}$ from the ionised Fe absorption line EWs, and a shell width (Paper I) of $\sim 10^{16}$ cm. Comparison with a density of $\sim 5 \times 10^5$ cm $^{-3}$ deduced from variability in the oxygen RRC (Paper II) would support the interpretation of co-moving ionised O and Fe flow components in pressure equilibrium with a temperature of 0.03 keV (from RRC widths) for the less ionised gas. A further implication of the inhomogeneous co-moving flow is that the ionisation parameters will differ in the ratio of the densities. While that ratio is somewhat less than the factor ~ 10 predicted for dominant O VIII and Fe XXV ion stages, the agreement is not unreasonable given the approximate nature of the above estimates.

7.1 A transient high velocity wind in NGC 4051

In Paper I we noted that absorption in the immediate post-shock gas, observed at velocities up to $v \sim 9000$ km s $^{-1}$ and ionisation parameter to $\log \xi \sim 3$, implied the presence of a still higher velocity wind, with $v \sim 36000$ km s $^{-1}$ and $\log \xi \sim 3.6$. Although the evidence presented in Paper I for such a highly ionised wind was marginal, we noted the Tombesi et al. (2010) report of the detection of an outflow at $\sim 0.13c$ ($v \sim 39000$ km s $^{-1}$) in the 2002 *XMM-Newton* observation of NGC 4051. We have repeated the 2002 data analysis in Section 6, finding the ~ 8 keV absorption to be the only significant absorption line in the Fe K spectral region, with its detection after 2 weeks of extreme low continuum flux being consistent with an increased fraction of Fe XXVI in a highly ionised wind.

The *Chandra* and *Suzaku* observations of NGC 4051, some 6 months prior to the 2009 *XMM-Newton* campaign, yielded absorption spectra showing no strong evidence in the soft X-ray band for outflow velocities $\gtrsim 1000$ km s $^{-1}$ (Lobban et al. 2011). Although the *Chandra* spectra are somewhat less sensitive, it seems clear that the soft X-ray opacity at ~ 3000 - 9000 km s $^{-1}$ was significantly weaker than 6 months later. On the other hand, the simultaneous *Suzaku* spectra did show a pair of strong absorption lines at ~ 6.8 and ~ 7.1 keV, interpreted - as here - with He- and H-like Fe, with a projected outflow velocity of ~ 5000 - 7000 km s $^{-1}$, but found no evidence for a higher velocity wind.

An obvious way of reconciling the 2008 and 2009 data is that the high velocity wind was weaker during the earlier observation, leading to a lower opacity in the post-shock flow. The flow speed and recombination timescales we have deduced (Paper II, and herein) would readily allow for that different picture over a 6-month interval. In particular, a denser (more massive) post-shock flow evidenced by the strong ~ 3000 - 7000 km s $^{-1}$ absorbing flow seen in the RGS spectrum of 2009 would support an assumption that the fast wind was also blowing more strongly in 2009 than during the *Chandra* and *Suzaku* campaign.

Emission from the pre-shock wind might be expected as a more persistent excess to the red wing of the absorption line at ~ 8 keV. However, for a spherical shell moving at $v \sim 0.13c$, any such feature would probably be correspond-

ingly broad and difficult to detect. A near-sided conical flow as indicated in the RGS data (Paper II) would give a less broad feature and it is interesting to note the excess near ~ 7.8 keV in figure 4. Adding a positive Gaussian to that fit, with a width $\sigma \sim 0.2$ keV, matches that excess and also enhances the absorption line depths at ~ 7.75 and ~ 8 keV. The corresponding forward cone semi-angle is $\sim 45^\circ$, similar to that deduced from the RGS spectral analysis in Paper II and optical imaging of NGC 4051 (Christopoulou et al. 1997).

In general, we might expect the putative, highly ionised fast wind in NGC 4051 to be intermittent, with the required super-Eddington condition for continuum driving (King and Pounds 2003) varying on the short (viscous or thermal) timescale of the inner disc. In that context it is important to note the very high column density required to detect a blue-shifted Fe K absorption line in a low redshift source such as NGC 4051, while radial expansion could rapidly render undetectable the line-of-sight column density in an initially optically thick transient outflow. Furthermore, the absence of the ~ 8 keV absorption line in rev 1730 (and rev 0263) is consistent with the line-of-sight component of the putative pre-shock wind (seen in FeXXVI Lyman- α) being more completely ionised by the stronger continuum $\gtrsim 7$ keV.

8 SUMMARY

Combining the pn data over the 600ks *XMM-Newton* observation of NGC 4051 shows a complex Fe K profile which can be resolved into both narrow and broad (red wing) emission components and several absorption lines. The narrow Fe K emission line has a mean energy consistent with fluorescence from weakly ionised matter and a line width consistent with scattering from the outflow seen in absorption.

Four blue-shifted absorption lines can be identified with Fe XXV and Fe XXVI resonance transitions consistent with line-of-sight outflow velocities separated by a factor ~ 4 , as expected for a fast highly ionised wind being shocked on impact with the ISM or slower moving ejecta.

Comparing Fe K profiles for individual orbits reveals significant changes on a few-day timescale, with the clear evidence for variations in the ionisation state of the post shock flow. While no strong correlation of absorption with continuum flux levels is found for all 15 observations over 45 days, shorter term trends strongly suggest a link of ionisation state with the soft X-ray (and UV) flux and - for the brightest orbit (rev 1730) - with a factor 2 increase in hard X-ray flux. While the former link is important in offering support for the existence of shocked gas which is being cooled by disk photons, the rapid response to a pulse of ionising radiation can be interpreted in terms of a recombination timescale which yields an electron density of $\sim 1.5 \times 10^5$ cm $^{-3}$. Comparison with the somewhat higher density derived in Paper II from the RGS spectral analysis is consistent with two ionisation components in a co-moving flow.

Finally, we confirm an absorption line at ~ 8 keV in the 2009 summed spectrum, at a similar energy and EW to that found in the 2002 data as part of the Tombesi et al. (2010) survey, and identified there with an outflow velocity of $\sim 0.13c$. In our more extended 2009 observations we find evidence that the ~ 8 keV line is variable, being stronger

when the flux level is lower. The implication is that the fast wind is very highly ionised at moderate or high continuum flux levels, with Fe predominantly in Fe XXVII. Recombination to Fe XXVI (see possible RRC in figure 1) would then increase the wind opacity when the ionising flux level fell. We recall that a fully ionised wind is quite likely in the continuum driving model of Black Holes Winds discussed by King and Pounds (2003).

Vaughan S., Uttley P., Pounds K.A., Nandra K., Strohmeyer T.E., 2011, MNRAS, 413, 2489

ACKNOWLEDGEMENTS

The results reported here are based on observations obtained with *XMM-Newton*, an ESA science mission with instruments and contributions directly funded by ESA Member States and the USA (NASA). We acknowledge illuminating discussions with Andrew King.

REFERENCES

- Alston W.N., Vaughan S., Uttley P., 2012 MNRAS, to be submitted
- Arnaud K.A., 1996, ASP Conf. Series, 101, 17
- Cappi M., 2006, Astron. Nachr., 327, 1012
- Christopoulou P.E., Holloway A.J., Steffen W., Mundell C.G., Thean A.H.C., Goudis C.D., Meaburn J., Pedlar A., 1997, MNRAS, 284, 385
- Chartas G., Brandt W.N., Gallagher S.C., Garmire G.P., 2002, ApJ, 569, 179
- Collinge M.J. et al. 2001, ApJ, 557, 2
- Done C., Mulchaey J.S., Mushotzky R.F., Arnaud K.A., 1992, ApJ, 395, 275
- Fabian A.C., Rees M.J., Stella L., White N.E., 1989, MNRAS, 238, 729
- Ferrarese L., Merritt D., 2000, ApJ, 539, L9
- Gebhardt K., et al. 2000, ApJ, 539, L13
- Haring N., Rix H-W., 2004, ApJ, 604, L89
- Hurkett C.P., et al. 2008, ApJ, 679, 587
- Kallman T.R., Palmeri P., Bautista M.A., Mendoza C., Krolik K.H., 2004, ApJS, 55, 675
- King A.R., 2003, ApJ, 596, L27
- King A.R., 2005, ApJ, 635, L121
- King A.R., Pounds K.A. 2003, MNRAS, 345, 657
- King A.R., 2010, MNRAS, 402, 1516
- King A.R., 2010a, MNRAS, 408, 95
- Lobban A.P., Reeves J.N., Miller L., Turner T.J., Braitto V., Kraemer S.B., Crenshaw D.M., 2011, MNRAS, 414, 1965
- Magdziarz P., Zdziarski A.A., 1995, MNRAS, 273, 837
- Matt G., 2002, MNRAS, 337, 147
- Pounds K.A., Reeves J.N., King A.R., Page K.L., O'Brien P.T., Turner M.J.L., 2003, MNRAS, 345, 705
- Pounds K.A., Reeves J.N., Page K.L., O'Brien P.T., 2004, ApJ, 616, 696
- Pounds K.A., Page K.L., 2006, MNRAS, 372, 1275
- Pounds K.A., Reeves J.N., 2009, MNRAS, 397, 249
- Pounds K.A., Vaughan S., 2011, MNRAS, 413, 1251 (Paper I)
- Pounds K.A., Vaughan S., 2011a, MNRAS, 415, 2379 (Paper II)
- Reeves J.N., O'Brien P., Ward M.J., 2003, ApJ, 593, L65
- Steenbrugge K.C., Fenovcik M., Kaastra J.S., Costantini E., Verbunt F. 2009, A&A, 496, 107
- Strüder L., et al. 2001, A&A, 365, L18
- Tombesi F., Cappi M., Reeves J.N., Palumbo G.G.C., Yaqoob T., Braitto V., Dadina M., 2010, A&A, 521, 57
- Turner M.J.L., et al. 2001, A&A, 365, L27
- Turner T.J., Miller L., 2010, ApJ, 709, 1230